The Journal of International Advanced Otology

J Int Adv Otol 2021; 17(2): 134–44 • DOI: 10.5152/JIAO.2021.0058

Original Article

Morphological Observations of the Bony Canal Structure of the Eustachian Tube in Elderly Human Cadavers With Cone-Beam Computed Tomography and Principal Component Analysis

Rieko Asaumi[1,*], Iwao Sato[2,*], Taisuke Kawai[1], Shinichi Kawata[2], Takuya Omotehara[2], Shintaro Kondo[3], Masahiro Itoh[2,*]

[1]Department of Oral and Maxillofacial Radiology, School of Life Dentistry at Tokyo, The Nippon Dental University, Chiyoda-ku, Tokyo, Japan
[2]Department of Anatomy, Tokyo Medical University, Shinjuku-ku, Tokyo, Japan
[3]Department of Anatomy, School of Dentistry at Matsudo, Nihon University, Matsudo, Chiba, Japan

Cite this article as: Asaumi R, Sato I, Kawai T, *et al*. Morphological observations of the bony canal structure of the eustachian tube in elderly human cadavers with cone-beam computed tomography and principal component analysis. *J Int Adv Otol.* **2021; 17(2): 134–44**.

OBJECTIVE: Anatomical information regarding the eustachian tube (ET) is limited; therefore, more detailed analytical data on ET structure is needed when planning surgical treatments involving the temporal bone.

METHODS: We examined the bony structure of the middle ear and ET in 30 Japanese donor cadavers (71-97 years old at the time of death) both macroscopically and with cone-beam computed tomography. Each ET was reconstructed in 3 dimensions, and the structure and correlations of ET element measurements, identified via principal component analysis, were analyzed.

RESULTS: Delineation between bony and cartilaginous zones appeared unclear, and the space between ET cartilage and the carotid canal was narrow. We observed stenosis of the ET bony canal in 43.3% of the specimens ($n = 30$). In 50% of the specimens, the position of the ET bony canal was depressed at the pharyngeal orifice of the auditory side of the tube, and the middle region was a roundish structure. The lateral and central regions of the bony canal were related to the ET bony canal structure.

CONCLUSION: The close proximity of the ET bony canal to the carotid canal is an important anatomical and morphological finding. Pre-surgical 3D modeling of the middle ear structure, or at a minimum, of the central region of the middle ear canal, may provide useful information for planning procedures that involve the ET.

KEYWORDS: Eustachian tube, canal for tensor tympani, carotid canal, CBCT, PCA

INTRODUCTION

The eustachian tube (ET), also called the auditory tube or the pharyngotympanic tube, is composed of a bony and cartilaginous canal that connects the middle ear to the nasopharynx; the structure of the cartilage is important, but the structure of the bone is critical for the functions of the ET. Maintaining correct middle ear pressure is essential for normal functioning of the middle ear receptors (tympanic plexus) and the ET.[1] Furthermore, the bony structure of the ET is an important part of the neural system associated with auditory function. Therefore, detailed data on ET bony canal (ETBC) structures are needed.

Examinations and analysis of the temporal bone and lateral skull base in surgical planning for clinical treatment have been previously performed using magnetic resonance imaging (MRI),[2] computed tomography (CT),[3,4] and cone-beam computed tomography (CBCT).[4-6] Moreover, 3-dimensional (3D) models from CT and MRI data have been used to analyze types of malformations of the human inner ear.[7] In clinical treatments, CBCT images have also been used for middle ear reconstruction.[4,5] CBCT analysis provides useful information on the structure of the temporal bone.[4]

*These authors contributed equally to this work.

Corresponding author: Rieko Asaumi, e-mail: asaumi-r@tky.ndu.ac.jp
Received: December 29, 2020 • **Accepted:** January 20, 2021
Available online at www.advancedotology.org

The magnitude of ET dilation during swallowing,[8] physiological ear clicks with deglutition or during other pharyngeal movements,[9] and the ciliary motion of the mucosa[10] have been reported. The extended length of the supratubal recess is mostly related to the prolonged bony part and the inwardly bending cartilaginous part of the ET in the early stages.[11] Calcification of ET cartilage and atrophy of the tensor veli palatini are closely associated with aging and are predisposing factors for ET dysfunction in older adults, based on histological observations of cadavers ranging in age from 2 days to 88 years (at the time of death).[12] The angle between the cartilaginous and bony portions is related to aging and the relative growth of the face, based on the 3D reconstruction of histological data from patients ranging in age from 3 months to 88 years.[13] Although ET size also varies with growth and age, data on how the bony region of the ET varies with age are lacking.

The increasing use of CBCT techniques on the skull base may possibly be because of surgeons' improved understanding of the complexity of skull base anatomy. Clinical instruments are selected by the surgeon based on the identification and management of various skull base structures. Balloon dilatations of the ET have been conducted despite the risk to safety from the carotid artery's proximity to the ET.[14-16]

Cluster analysis, using the average linkage between groups (hierarchical cluster analysis algorithms) based on the significant components of principal component analysis (PCA), has been performed on biological data.[17] Recently, PCA data were closely related to biological parameters such as glucose, insulin, and C-peptide levels, age, BMI,[18,19] and cell identities.[20] The usefulness of PCA on CBCT data has also been demonstrated.[21,22] Multivariate modeling uses quantitative PCA data to estimate the interaction among variables such as CBCT measurements, age, and sex. Detailed data on the temporal bone region of the ET, such as CBCT images of the temporal bone and identification of the relationship between the ET and other elements of the middle ear using PCA, could provide useful information for surgical treatments of the skull.

METHODS

Specimens

A total of 30 Japanese donor cadavers (age at death 71-97 years, mean 86.2, SD 7.8) from Nippon Dental University and Tokyo Medical University were used in this study. The sample comprised 10 male cadavers (age at death 74-90 years, mean 82.7, SD 5.8) and 20 female cadavers (age at death 71-97 years, mean 87.9, SD 8.2).

Macroscopic Observations

Dissection, at a macroscopic level, was conducted on 4 cadavers to view the pharyngeal orifice of the ET inside the nasal cavity ($n = 2$) and the lateral side of the temporal bone from the external ear canal ($n = 2$).

CBCT Imaging

CBCT imaging of the temporomandibular joint was performed using an AZ 3000CT scanner (Asahi Roentgen Industry, Kyoto, Japan). Images of the ETBC and surrounding structures were also acquired. From 3D CBCT images (tube potential = 85 kV; tube current = 4 mA; cylindrical scan region: 79 mm diameter × 71 mm height; resolution: high; voxel size = 0.155 mm), the diameter of the skull was measured using Mimics Innovation Suite for Research (Materialize, Leuven, Belgium) and Micro AVS version 11 (KGT Industry, Tokyo, Japan) software. The median sagittal plane and the Frankfort plane were defined as vertical and horizontal reference planes. The vertical height (MH) and horizontal width (MW) of the ETBC at the middle ear, the vertical height (CH) and horizontal width (CW) at the middle canal center, and the vertical height (PH) and the horizontal width (PW) of the ETBC at the nasopharynx were measured (see Figure 1). The anterior-posterior length of the ETBC (LETBC), the minimum distance between the carotid canal and the ETBC (DCA), the vertical angle of the median sagittal plane (VA), and the horizontal angle of the Frankfort plane (HA) were also measured. We classified ETBC density as fine or blurry images and the border between the ETBC and tensor tympani as fine or blurry (see Figure 1).

Statistical Methods

CBCT measurements were analyzed using a 2-way analysis of variance (ANOVA) and post hoc Bonferroni test with 1 categorical independent variable and 1 continuous variable. Pearson coefficients were calculated to determine correlations. The level of significance was set as $P < .05$. PCA was performed on each individuals' data.[17,18] Multivariate modeling of quantitative PCA data was used to estimate interactions among CBCT measurements, age, and sex. We performed cluster analysis using the average linkage between groups (hierarchical cluster analysis algorithms) and statistically significant principal components. Statistical analyses were performed using SPSS Statistics Base version 22 (IBM Corp, Armonk, NY, USA).

RESULTS

Macroscopic Observation

After removing soft tissue and some pieces of bone from the inferior region of the middle ear, the ET, the ET cartilage, and the auditory ossicles were visible (Figure 1). The cartilage surrounded the pharyngeal orifice. The bone appeared to overlie the cartilage from the middle of the cartilaginous part. Dissection of the temporal bone from the external ear canal revealed that a structure of connective tissue. However, the border between the bone and cartilage was unclear, and the space between the ET cartilage and the carotid artery was very narrow (Figure 2).

CBCT Analysis

ETBCs were defined and classified according to 3 shapes: a funnel narrowing toward the pharyngeal orifice (FS, $n = 21$; 35%), a depressed shape (DS, $n = 21$; 35%), and canal stenosis (CCS, $n = 18$; 30%) (Figure 3, Table 1). The middle region of the ETBC was classified as type 1 (flat, $n = 9$; 15%), type 2 (round, $n = 30$; 50%), and type 3 (depressed, $n = 21$; 35%) (Figure 4, Table 1). The internal density of the bone canal (Figure 1) was fine in 53% ($n = 32$) and blurry in 47% ($n = 28$) of images. The border between the ETBC and the canal for the tensor tympani (Figure 1) was fine in 75% ($n = 45$) and blurry in 25% ($n = 15$) of images.

Correlations among ETBC Measurements

Significant positive correlations were found between age and gender ($r = 0.322$, $P < .05$), ETBC structure type and CW ($r = 0.377$, $P < .01$), MW and CW ($r = 0.379$, $P < .01$), PW and CW ($r = 0.348$, $P < .01$),

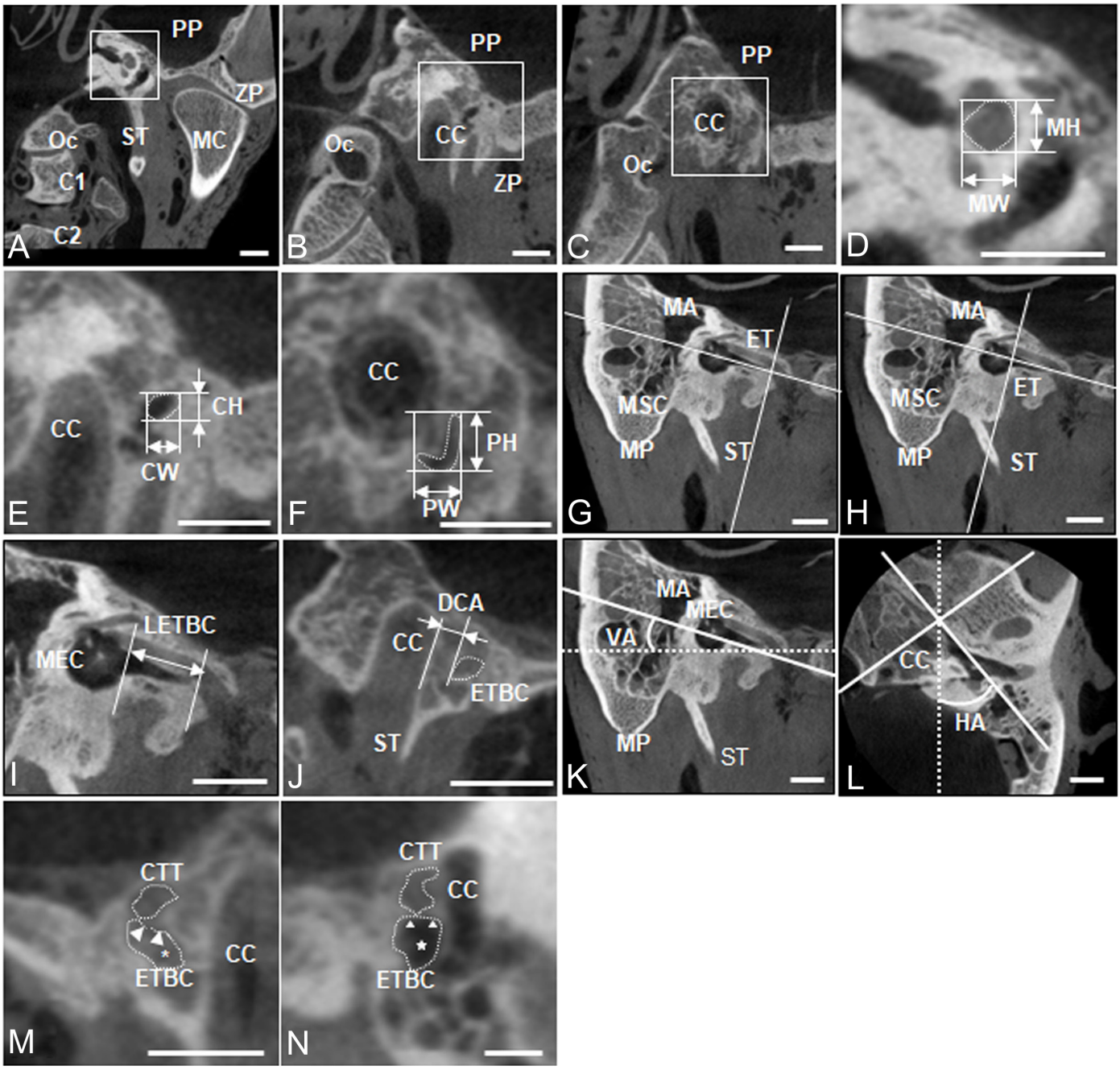

Figure 1. (a) Coronal image of the middle ear side of the ETBC; (b) coronal image of the antero-posteriorly center of the ETBC; (c) coronal image of the pharyngeal side of the ETBC. Measurement points of the vertical height (MH) and horizontal width (MW) of the middle ear side of the ETBC (d); the vertical height (CH) and horizontal width (CW) of the antero-posteriorly center of the ETBC (e); and the vertical height (PH) and horizontal width (PW) of the pharyngeal side of the ETBC (f). (d–f) are magnified images of the square section of a, b and c. The dotted line in (d-f)indicates the ETBC. Measurement points of the anterior-posterior length of the bony Eustachian tube (LETBC) are shown in g to i. (g) Anterior points (vertical line); (h) posterior point (vertical line); (i) Figures at a higher magnification. g and h; j, measurement points of the minimum distance between the bony ETBC (dotted oval line) and the carotid canal (CC) (DCA); k, measurement points of ETBC structures in the vertical angle to the Frankfort plane (VA); l, the horizontal angle to the median sagittal plane (HA); k, the dotted line is parallel to the Frankfort plane; l, the dotted line is parallel to the median sagittal plane; m and n, defined bone density images of ETBC such as fine (white star) and blurry (asterisk) images and border bony images between the ETBC and tensor tympani (CTT) as blurry (arrow) and fine (white arrowheads). C1, first cervical vertebra; C2, second cervical vertebra; CC, carotid canal; MC, mandibular condyle; Oc, Occipital bone; PP, petrous portion; ZP, zygomatic portion; ST, styloid process; ET, eustachian tube; LETBC, anterior-posterior length of the ET of the bony canal; ETBC, ET of the bony canal; VA, vertical angle of the ETBC; and HA, the horizontal angle of the ETBC; CC, carotid canal; MA, mastoid antrum; MEC, middle ear cavity; MSC, mastoid air cell; MP, mastoid process; CTT, canal for tensor tympani, Bar = 1 cm. C1, first cervical vertebra; C2, second cervical vertebra; CC, carotid canal; MC, mandibular condyle; Oc, Occipital bone; PP, petrous portion; ZP, zygomatic portion; ST, styloid process; ET, eustachian tube; LETBC, anterior-posterior length of the ET of the bony canal; ETBC, ET of the bony canal; VA, vertical angle of the ETBC; and HA, the horizontal angle of the ETBC; CC, carotid canal; MA, mastoid antrum; MEC, middle ear cavity; MSC, mastoid air cell; MP, mastoid process; CTT, canal for tensor tympani, Bar = 1 cm

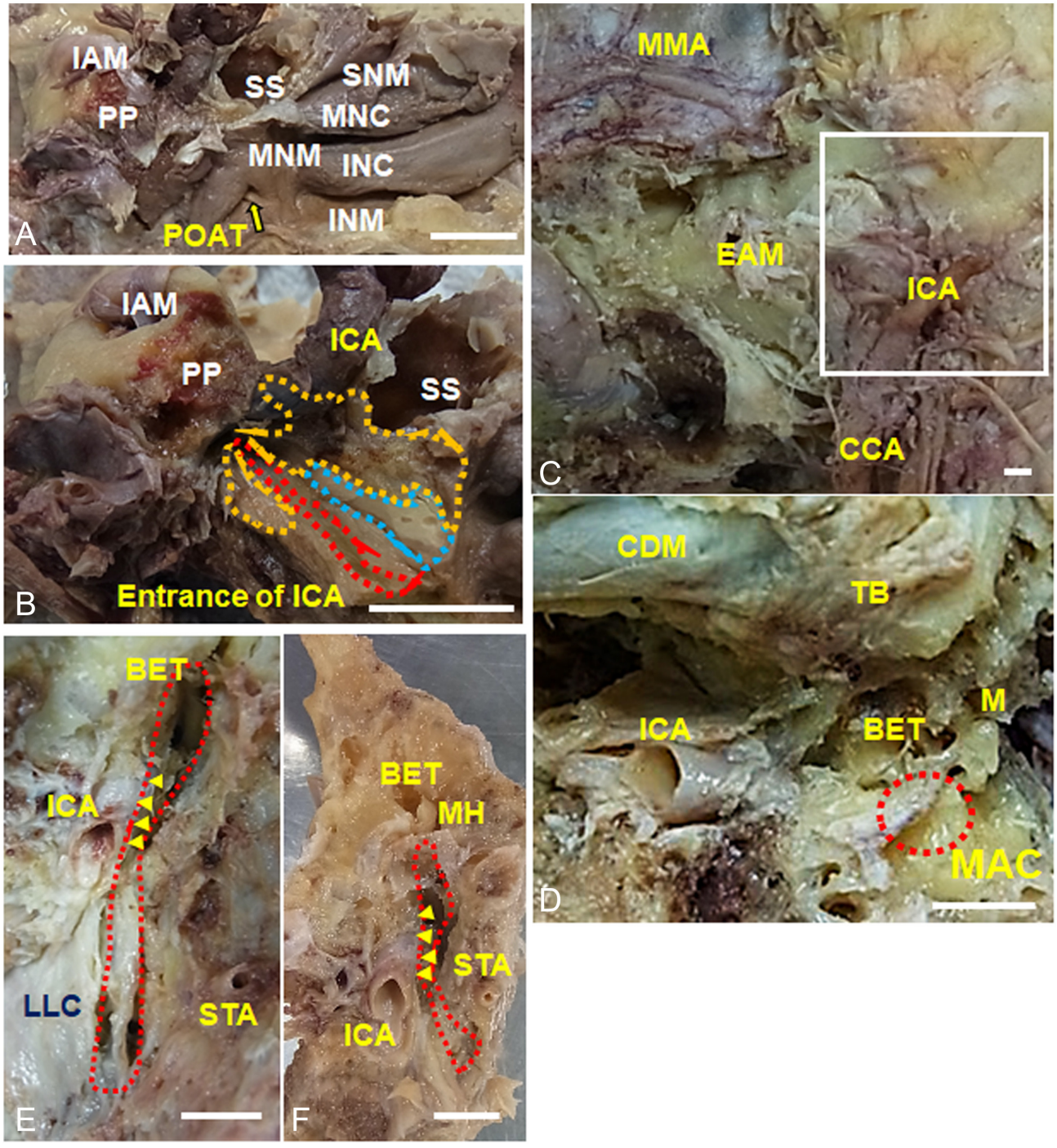

Figure 2. The pharyngeal orifice of the ET is viewed from the inside of the nasal cavity. After removing the soft tissue and some bones of the inferior region of the middle ear around the entrance of the ET, including the ET, the ET cartilage (CAT) and the auditory ossicles (yellow dotted line area) are visible. The middle ear is not seen in this figure (a, b). The CAT is located around the ET (red dotted line area) at the pharyngeal orifice of the ET side (arrow). The bony part (orange dotted line area) appears to cover the cartilage (blue dotted line area) from the middle of the cartilaginous part. The outer side of this bony ET eventually loses cartilage just before the middle ear and there is a transformation to the bone from cartilage (a, b). The border between the bony and cartilaginous zones is unclear, and the narrow space between the ET cartilage and carotid artery (arrowheads) should be noted (a, b). In the dissection from the outside of the temporal bone (c, d), the middle ear appears except for the bony part constituting the external ear canal, and the ET covered with the bony part can be seen below the middle ear (d). Furthermore, excluding this bone (red circle), the ear canal forms a structure of connective tissue (e, f). BET, bony part of ET; CAT, cartilage of ET; CCA, common carotid artery; CDM, cerebral dura mater; EAM, external acoustric; IAM, internal acoustics meatus; ICA, internal carotid artery; INM, Inferior nasal meatus; LLC, ligament of longus capitis; MAC, mastoid air cells; M, malleus; MH, malleus head; MMA, middle meningeal artery; MNC, middle nasal concha; MNM, middle nasal meatus; POAT, pharyngeal orifice of ET; PP, petrous part; SNM, superior nasal meatus; STA, superficial temporal artery; TB, temporal bone, SS, sphenoidal sinus, Bar = 1 cm.

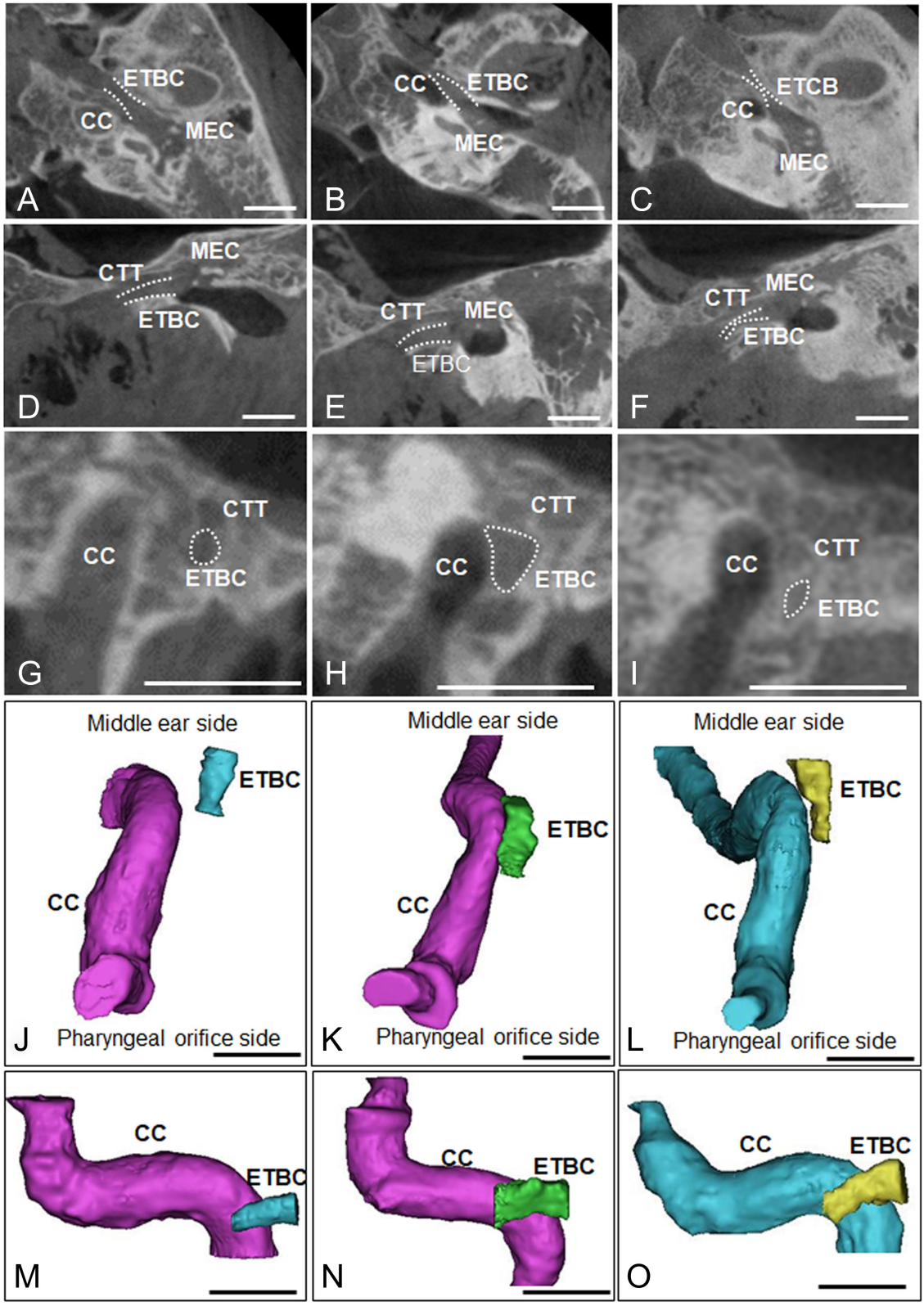

Figure 3. The ETBC structures were defined and classified into 3 different shapes: a shape where the funnel narrows toward the pharyngeal orifice of the ET (FS), a depressed shape (DS), and a shape with canal stenosis (CSS). a, d, g, j and m = images of type FS; b, e, h, k and n = images of type DS; c, f, I, l and o = images of type CSS; a, b, and c = axial section; d, e, and f = sagittal section; g, h, and i = coronal section; j, k, and l = upper view of 3-dimensional structural images of the ETBC; m, n and o = lateral view of 3-dimensional structural images of the ETBC. ETBC, ET of the bony canal; MEC, middle ear cavity; CC, carotid canal; CTT, tensor tympani; Bar = 1 cm.

Table 1. The Morphological Classification of the ETBC. The 3D Shape of the ETBC and the Cross-Sectional Shape of Middle Region of the ETBC

3D shape of ETBC structure	FS	DS	CSS	Total
Sides	21 (35%)	21 (35%)	18 (30%)	60
Shape of middle region of ETBC	**Type 1**	**Type 2**	**Type 3**	**Total**
Sides	9 (15%)	30 (50%)	21 (35%)	60

The 3-dimensional structures of the ETBC were defined and classified into 3 different shapes: a shape where the funnel narrows toward the pharyngeal orifice of the ET (FS), a depressed shape (DS), and a shape with canal stenosis (CSS) in Figure 3.
The cross-sectional shape of the middle region of the ETBC (vertical lines) in Figure 4 was defined as flat (type 1), round (type 2).

CH and MH (r = 0.305, $P < .05$), CH and PH ($r = 0.279$, $P < .05$), MH and ETBC structure type ($r = 0.319$), PH and MH ($r = 0.310$), PW and bone density ($r = 0.284$, $P < .05$), and PW and PH ($r = 0.419$, $P < .01$). A significant negative correlation was found between gender and LETBC ($r = –0.485$, $P < .01$) and CW and DCA ($r = –0.355$, $P < .01$). Correlations and measurement data (mean and SD) are shown in Table 2.

PCA and Cluster Analysis

Projections of the 15 variables in a 2-dimensional space defined by the 2 axes of component 1 (*x*-axis) and component 2 (*y*-axis) are shown in Figure 5. The 2 principal components significantly explained 27.7% (component 1: 15.8%; component 2: 11.9%) of the information in the data set. Clustering analysis using a hierarchical classification model with these components demonstrated that optimal grouping with 2 clusters (Figure 5). The contributions of ETBC widths and structure (CW, 0.751; PW, 0.441; MW, 0.407, structure, 0.601) are explained by component 1. The contributions of the other ETBC measurement elements (CH, 0.607; PH, 0.597; MH, 0.418; DCA, –0.406) are represented by component 2 (see Table 2).

DISCUSSION

In general, the ET plays an important role in equalization, oxygenation, and drainage of the tympanic cavity in the middle ear; its structure provides a controlled air exchange in the tympanic cavity or provides an outlet for mucus and other fluid from the middle ear to the nasopharynx.[23] The ET is composed of bone, cartilage, and connective tissue. Based on data from 10 cadavers, Brown et al.[24] reported the mean distance from the nasopharynx to the ET genu was 23 mm (SD 5 mm), the mean distance from the ET genu to the anterior aspect of the tympanic membrane was 24 mm (SD 3 mm), and the mean total ET length was 47 mm (SD 4 mm). To cannulate the ET successfully and minimize the risk of harm, an understanding of ET anatomical structure is the most important factor.[24] In our macroscopic observation, the border between the bony zone and cartilage zone was unclear, and there was a very narrow border between the ET cartilage zone and the carotid artery. Attention must be paid to the carotid artery during cannulation and surgical treatments with an endonasal approach.

Skull base surgery requires more detailed anatomical information on the temporal bone.[2-5,25,26] Previous reports have examined the ET as part of the hearing system[6,8,25]; however, more detailed data and improved analysis are needed by surgeons.[2-5,25-27] In general, in pre-surgical planning, specific areas such as the petrous apex, suprapetrous area (i.e., above the petrous internal carotid artery), infrapetrous area (i.e., below the petrous internal carotid artery), and infratemporal fossa for the temporal bone and lateral skull base must be identified. From a posterior coronal approach, there are multiple areas, such as the foramen magnum, occipital condyle, hypoglossal canal, and jugular foramen, where the risk of neurosurgical injury is greater.[25,26] Therefore, in pre-surgical planning, the ET structure, with its bony parts, are important elements among the auditory compartments that must be considered.

Takasaki et al.[28] reported that the mean ET angle and length were 27° and 4.3 mm, respectively, based on an analysis of CT images ($n = 90$, age-range 18-82 years old). In contrast, our results, which showed that the mean ET angle and length were 18.4° (SD 5.1°) and 8.7 mm (SD 2.2 mm) in older adult human cadavers (see Table 2). This difference was as a result of different methods and measurement points used in the studies.

Hard tissue structures can be observed in detail with CBCT. Though the size of a CBCT device is smaller than that of a multi-detector row CT device and the price of a CBCT device is cheaper than that of a multi-detector row CT, with CBCT images it is difficult to observe soft tissues and impossible to calculate CT units. In general, CBCT has been explored for applications in endodontic surgical planning, and dentoalveolar trauma evaluation.[29] Recently, CBCT has been used to image bony structures of the anterior and lateral skull base because the radiation dose of CBCT is lower than that of CT.[30,31] Peltonen et al.[32] suggested that CBCT images were at least equivalent to those from multi-detector row CT. Kemp et al.[4] also described high-quality images and low-dose radiation when using CBCT for the middle ear. Therefore, the CBCT images of the temporal bone can be used for general diagnosis. Our CBCT images clearly showed the 3D structure of the ETBC, and our analysis demonstrated correlations between bone structures.

The morphological features of the ETBC structure are important for temporal bone treatments. In general, the chorda tympani nerve and the auricular branch arise from the facial nerve and run through the tympanic or horizontal area in the facial nerve canal. The tympani nerve is also tightly connected to the bony region of the ET. Therefore, more detailed information on the bony structure of the ET may also provide information on innervation. Our findings on the structure of the middle region of the ETBC (flat, round, or depressed) may contribute to the knowledge of chorda tympani innervation and that of the auricular branch. Moreover, the minimum distance between the carotid canal and the ETBC was negatively correlated with the CW (middle canal width). Therefore, precise information on the ETBC structure is important to identify where the chorda tympani nerve and the auricular branch lie.

Noonan et al.[33] reported that of the distances between the carotid artery and the cartilaginous ET, the bony-cartilaginous junction, and the ETBC, as well as the distance to the carotid canal, were narrowest at the ETBC in both children and adults. We found that the distance between the ETBC and carotid canal was narrow, ranging from 0 to 3.4 mm (mean 1.2 mm, SD 0.8 mm) (see Figure 5). The CBCT structure also reflected the minimum distance between the carotid canal and the ETBC at the pharyngeal orifice and the density between the tensor tympani and ETBC. ETBC width elements mainly contributed to

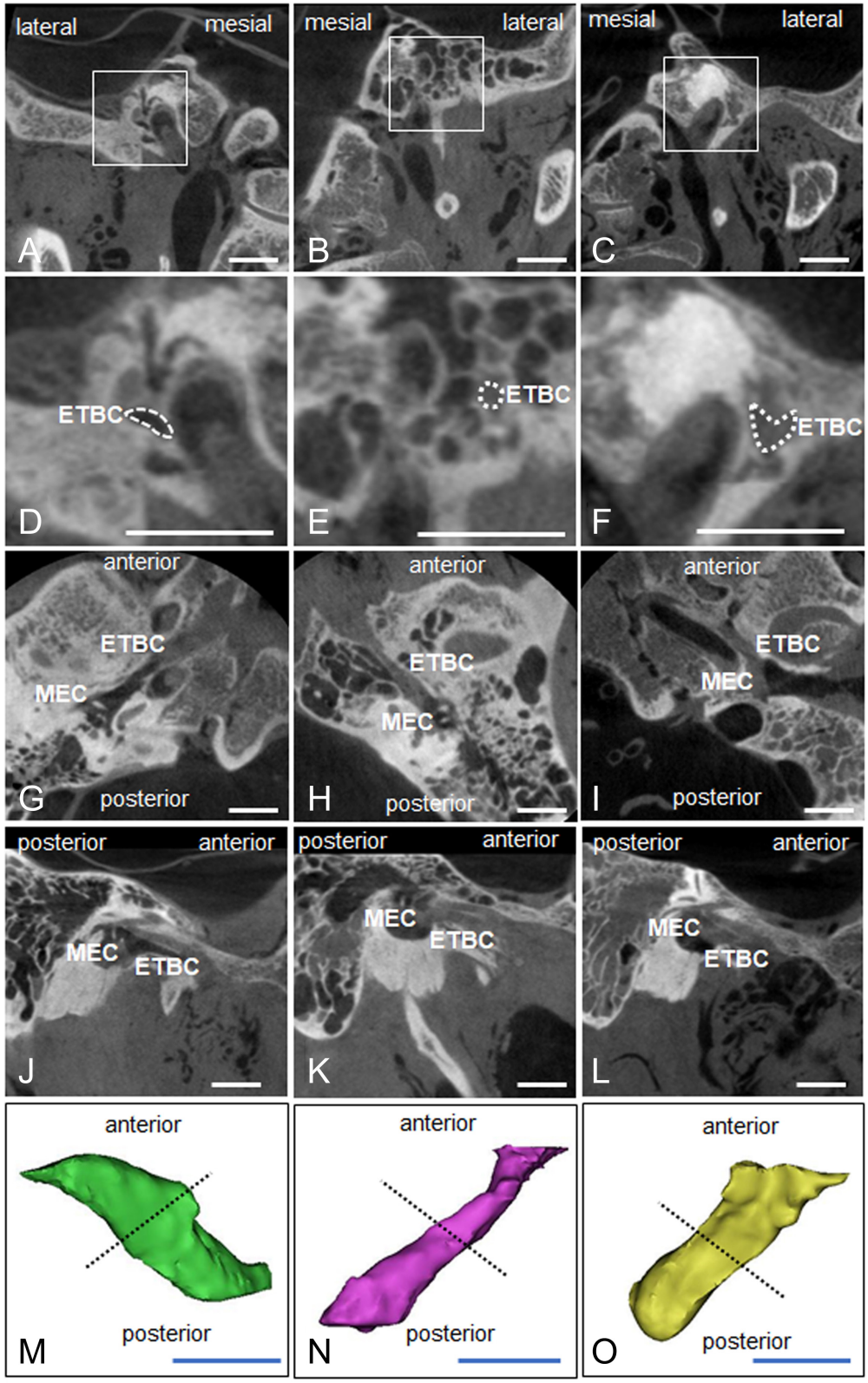

Figure 4. The middle region of the ETBC (vertical lines) in m, n, and o was defined as flat (type 1), round (type 2), or depressed (type 3). a, d, g, j and m = type 1; b, e, h, k and n = type 2; c, f, l, l and o = type 3. a, b, and c = coronal section; d, e, and f = images of the square sections of a, b and c seen at a higher magnification; g, h, and i = axial section; j, k, and l = sagittal section; m, n, and o = 3-dimensional structural images of the ETBC. ETBC, ET of the bony canal; MEC, middle ear cavity; Bar = 1 cm.

Table 2. Measurements Based on the CBCT Analysis Data From the Temporal Bone
(A) Correlation Coefficients Between CBCT Analysis Data From the Temporal Bone

	Aging	Gender	RL	Stru	Density	Border	HA	VA	MH	MW	PH	PW	CH	CW	PTL	DCA
Aging	1															
Gender	0.322*	1														
RL	0.000	0.000	1													
Stru	−0.023	0.030	0.104	1												
Border	0.135	−0.163	−0.115	0.109	−0.154	1										
HA	−0.151	0.149	0.077	−0.036	0.034	−0.017	1									
VA	0.050	−0.120	−0.253	0.149	−0.011	0.201	−0.012	1								
MH	0.143	0.160	−0.046	0.319*	−0.183	.0054	−0.073	−0.211	1							
MW	0.014	−0.128	−0.065	0.232	0.035	0.088	0.040	0.100	0.216	1						
PH	0.143	0.109	0.041	0.134	0.149	−0.078	−0.210	0.027	0.310*	−0.053	1					
PW	0.105	−0.182	0.045	0.176	−0284*	0.087	−0.118	0.094	−0.228	0.131	0.419**	1				
CH	0.010	−0.090	−0.071	0.173	0.003	0.082	−0.121	−0.064	0.305*	0.144	0.279*	0.060	1			
CW	−0.079	−0.046	0.044	0.377**	0.013	−0.074	−0.048	0.046	0.045	0.379**	0.273*	0.348**	0.383**	1		
PTL	−0.007	−0.485**	0.012	−0.180	−0.224	0.151	−0.091	−0.114	−0.101	0.119	−0.113	0.079	−0.222	−0.084	1	
DCA	0.044	−0.071	−0.162	−0.151	0.009	0.169	−0.067	0.075	0.013	−0.068	−0.094	−0.070	−0.149	−0.355**	0.184	1

*$P < .05$, **$P < .01$.

Aging (difference of aging), gender (difference of gender), RL (difference of right and left sides), Stru (inner structure of ETBC (eustachian tube bony canal)), border (border bony images between the ETBC and tensor tympani), HA (horizontal angle to the median sagittal plane), VA (vertical angle to the Frankfort plane), MH (vertical height of the middle ear side of the ETBC), MW (horizontal width of the middle ear side of the ETBC), PH (vertical height of the pharyngeal side of the ETBC), PW(horizontal width of the pharyngeal side of the ETBC), CH (vertical height of antero-posteriorly center of the ETBC), CW (horizontal width of antero-posteriorly center of the ETBC), PTL (pharyngotympanic tube length = LETBC: anterior-posterior length of the ETBC), DCA (minimum bony distance between ETBC and the carotid canal).

(B) Measurement Data of ET Elements (Average and SD)

	HA	VA	MH	MW	PH	PW	CH	CW	PTL	DCA
Average	47.2	18.0	3.92	4.40	3.18	2.89	2.71	3.04	8.32	5.76
SD	7.84	5.52	1.06	1.00	0.96	0.93	0.67	0.79	2.27	1.56

HA and VA, angle; MH-DCA, mm.
HA (horizontal angle to the median sagittal plane), VA (vertical angle to the Frankfort plane), MH (vertical height of the middle ear side of the ETBC), MW (horizontal width of the middle ear side of the ETBC), PH (vertical height of the pharyngeal side of the ETBC), PW (horizontal width of the pharyngeal side of the ETBC), CH (vertical height of antero-posteriorly center of the ETBC), CW (horizontal width of antero-posteriorly center of the ETBC), PTL (pharyngotympanic tube length = LETBC: anterior-posterior length of the ETBC), DCA (minimum bony distance between ETBC and the carotid canal).

the structure of the ETBC, and aging and gender elements also contributed to the ETBC length and height based on PCA. Therefore, the pharyngeal side of the elements is an important factor for the ETBC.

Robert et al.[34] reported that the shape of the bony part of the ET could be observed in CT imaging and that the ET fibrocartilaginous part could be imaged on CT but was more easily observed in MRI images. The ET cartilage is firmly attached to the skull base by lateral and medial suspensory ligaments, which are separated by the medial Ostmann fat pad.[35] In our macroscopic level dissection, a large part of the ET cartilage covered a bony structure at the narrow tunnel portion of the ET. This suggested that the cartilage was limited by bone remodeling during aging and growth. Therefore, the bony structure may have an effect on components such as cartilage, ligaments, and other connective tissues during aging.

Our PCA analysis showed 2 groups: the first group contained width, angle, and structural elements; whereas the second group contained aging, gender, asymmetry, and height elements. Two large elements, in the vertical and horizontal direction, affect the structure of ETBC. The horizontal length factors, those related to the width of ETBC (PW, MW, and CW), were inversely proportional to the angle of HA. This suggests that the smaller the HA angle is, the longer the horizontal axis of the ETBC will be. CH, PH, and MH were related to the vertical length of the ETBC and were inversely proportional to the distance between the carotid canal and the ETBC. In the vertical direction of the ETBC, the CH, PH, and MH elements are important regarding the length of the ETBC. In addition, gender and aging factors were inversely proportional to ETBC length, which suggests that ETBC shortens in the vertical direction with aging. The narrowing of the ETBC structure is also affected by remodeling in, at least, the vertical direction.

(C) Component Matrices Between CBCT Analysis Measurement Data of the Human Temporal Bone in Component 1 and Component 2

	Comp. 1	Comp. 2
CW	0.751	0.181
CH	0.607	−0.013
Stru	0.601	0.061
PH	0.597	−0.096
PW	0.441	0.406
DCA	−0.406	0.206
Gender	0.070	−0.787
PTL	−0.297	0.624
MH	0.418	−0.287
Border	−0.003	0.429
Aging	0.102	−0.209
HA	−0.179	−0.206
VA	0.047	0.368
RL	0.059	−0.181
MW	0.407	0.344

Aging (difference of aging), gender (difference of gender), RL (difference of right and left sides), Stru (inner structure of ETBC (eustachian tube bony canal)), border (border bony images between the ETBC and tensor tympani), HA (horizontal angle to the median sagittal plane), VA (vertical angle to the Frankfort plane), MH (vertical height of the middle ear side of the ETBC), MW (horizontal width of the middle ear side of the ETBC), PH (vertical height of the pharyngeal side of the ETBC), PW(horizontal width of the pharyngeal side of the ETBC), CH (vertical height of antero-posteriorly center of the ETBC), CW (horizontal width of antero-posteriorly center of the ETBC), PTL (LETBC: anterior-posterior length of the ETBC), DCA (minimum bony distance between ETBC and the carotid canal).

CONCLUSION

We have investigated detailed data in an analysis of the ET in 30 Japanese donor cadavers ranging from 71 to 97 years old using macroscopic, CBCT and PCA methods. The very narrow space between the ET cartilage and carotid artery in the ET, the ETBC, was classified into 3 types and the proximity position of the ETBC also indicated specific structures. These ETBC structure data by PCA and CBCT analysis were affected by remodeling of the middle ear side or the middle canal center side regions, and these data could give useful information at the anatomical level when planning surgical procedures involving the ET.

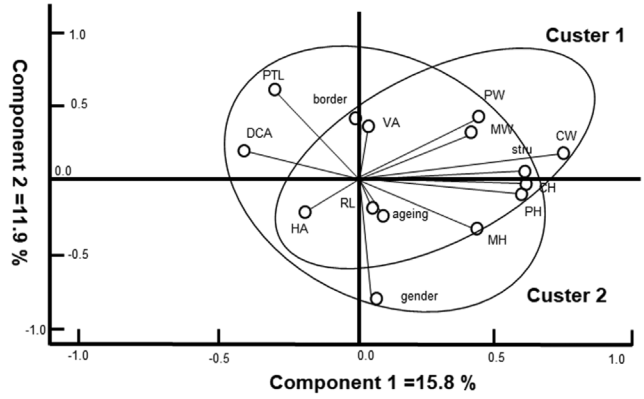

Figure 5. PCA analysis of the map in Cluster 1 and Cluster 2. We defined the 2 large groups as Cluster 1 and Cluster 2. We defined measurement data for the ETBC of the middle ear side of the vertical height (MH) and horizontal width (MW), middle canal center of the vertical height (CH) and horizontal width (CW), and pharyngeal side of the vertical height (PH) and horizontal width (PW) (see Figure 1); the anterior-posterior length of the ETBC (PTL (LETBC)), the vertical angle to the Frankfort plane (VA) and horizontal angle to the median sagittal plane (HA), and the minimum bony distance between the ETBC and the external acoustic meatus (DCA).

Ethics Committee Approval: This study was performed in line with the principles of the Declaration of Helsinki (as revised in 2013). The cadavers used in the present study were donated to Tokyo Medical University and Nippon Dental University, Tokyo, Japan, based on the Act on Body Donation for Medical and Dental Education. The study was approved by the Ethics Review Committee of Nippon Dental University (2018/21/ July; No. NDU-T2015-20) and Tokyo Medical University, Institutional Review Board (2019/01/March.; TMU, No. T2018-0060).

Informed Consent: All the donors willingly signed a form consenting to the body donation for education and research, and all the donors could revoke the intended donation any time without any disadvantages. The collection and use of the CBCT data of all the cadavers were carried out with the permission of the donors and their family, and then performed according to the Law Concerning Cadaver Dissection and Preservation enacted in Japan in 1949.

Peer-review: Externally peer-reviewed.

Authors Contributions: Concept - R.A., I.S., M.I.; Design - R.A., I.S., M.I.; Supervision - I.S., M.I; Materials - R.A.; Data Collection and/or Processing - R.A., I.S., T.K., S.K., T.O.; Analysis and/or Interpretation - R.A., I.S., S.K.; Literature Reviews - T.K.; Writing - R.A., I.S.

Acknowledgments: The authors thank the members of Department of Anatomy, School of Life Dentistry at Tokyo, the Nippon Dental University for their kind support in providing samples of this study. The authors thank Coren Walters-Stewart, PhD, and Edanz Group (https://en-author-services.edanz.com/ac) for editing a draft of this manuscript.

Conflicts of Interest: The authors declare that they have no competing interests.

Financial Disclosure: The authors declared that this study had received no financial support.

REFERENCES

1. Rinaldi V, Cappadona M, Gaffuri M, Torretta S, Pignataro L. Chorda tympani nerve, may it have a role in stabilizing middle ear pressure? *Med Hypo*. 2013;80(6):726-727. [CrossRef]
2. De Foer B, Vercruysse JP, Spaepen M, et al. Diffusion-weighted magnetic resonance imaging of the temporal bone. *Neuroradiology*. 2010;52(9):785-807. [CrossRef]
3. Prades JM, Elmaleh-Berges M, Chatard S, et al. Computed tomography of the normal and pathologic temporal bone. *Morphologie*. 2011;95(311):159-169. [CrossRef]
4. Kemp P, Stralen JV, De Graaf PD, et al. Cone-beam CT compared to multislice CT for the diagnostic analysis of conductive hearing loss: a feasibility study. *J Int Adv Otol*. 2020;16(2):222-226. [CrossRef]
5. Zaoui K, Kromeier J, Neudert M, et al. Clinical investigation of flat panel CT following middle ear reconstruction: a study of 107 patients. *Eur Radiol*. 2014;24(3):587-594. [CrossRef]
6. Güldner C, Diogo I, Bernd E, et al. Visualization of anatomy in normal and pathologic middle ears by cone beam CT. *Eur Arch Otorhinolaryngol*. 2017;274(2):737-742. [CrossRef]
7. Dhanasingh A, Dietz A, Jolly C, Roland P. Human inner-ear malformation types captured in 3D. *J Int Adv Otol*. 2019;15(1):77-82. [CrossRef]
8. Alper CM, Teixeira MS, Swarts JD. Correlations between videoendoscopy and sonotubometry of Eustachian tube opening during a swallow. *Laryngoscope*. 2016;126(12):2778-2784. [CrossRef]
9. Ehrt K, Fischer HG, Dahl R, et al. "Physiological" ear clicking: its origin and potential usability as a test tool for the Eustachian tube function. *Otol Neurotol*. 2016;37(4):345-349. [CrossRef]
10. Li Y, Liu H, Li J, et al. Morphology and ciliary motion of mucosa in the Eustachian tube of neonatal and adult gerbils. *PLoS ONE*. 2014;9(6):e99840. [CrossRef]
11. Hong J, Chen K, Lyu H, et al. Age-related changes in the morphological relationship between the supratubal recess and the Eustachian tube. *Auris Nasus Larynx*. 2018;45(1):88-95. [CrossRef]
12. Takasaki K, Sando I, Balaban CD, et al. Histopathological changes of the Eustachian tube cartilage and the tensor veli palatini muscle with aging. *Laryngoscope*. 1999;109(10):1679-1683. [CrossRef]
13. Ishijima K, Sando I, Balaban C, Suzuki C, Takasaki K. Length of the Eustachian tube and its postnatal development: computer-aided three-dimensional reconstruction and measurement study. *Ann Otol Rhinol Laryngol*. 2000;109(6):542-548. [CrossRef]
14. Poe DS, Silvola J, Pyykkö I. Balloon dilation of the cartilaginous Eustachian tube. *Otolaryngol Head Neck Surg*. 2011;144(4):563-569. [CrossRef]
15. Kepchar J, Acevedo J, Schroeder J, Littlefield P. Transtympanic balloon dilatation of Eustachian tube: a human cadaver pilot study. *J Laryngol Otol*. 2012;126(11):1102-1107. [CrossRef]
16. Jufas N, Treble A, Newey A, Patel N. Endoscopically guided transtympanic balloon catheter dilatation of the Eustachian tube: a cadaveric pilot study. *Otol Neurotol*. 2016;37(4):350-355. [CrossRef]
17. Cassar-Malek I, Passelaigue F, Bernard C, Léger J, Hocquette JF. Target genes of myostatin loss-of-function in muscles of late bovine fetuses. *BMC Genomics*. 2007;8:63. [CrossRef]
18. Göbl CS, Bozkurt L, Mittlböck M, et al. To explain the variation of OGTT dynamics by biological mechanisms: a novel approach based on principal components analysis in women with history of GDM. *Am J Physiol Regul Integr Comp Physiol*. 2015;309(1):R13-R21. [CrossRef]
19. Stopp T, Feichtinger M, Rosicky I, et al. Novel indices of glucose homeostasis derived from principal component analysis: application for metabolic assessment in pregnancy. *J Diabetes Res*. 2020;2020:4950584. [CrossRef]
20. Chung NC. Statistical significance of cluster membership for unsupervised evaluation of cell identities. *Bioinformatics*. 2020;36(10):3107-3114. [CrossRef]
21. Codari M, Zago M, Guidugli GA, et al. The nasal septum deviation index (NSDI) based on CBCT data. *Dentomaxillofac Radiol*. 2016;45(2):20150327. [CrossRef]
22. Terada K, Kameda T, Kageyama I, Sakamoto M. Estimation of three-dimensional long axes of the maxillary and mandibular first molars with regression analysis. *Anat Sci Int*. 2020;95(1):126-133. [CrossRef]
23. Savenko IV, Boboshko MY. The patulous Eustachian tube syndrome: the current state-of-the-art and an original clinical observation. Second communication. *Vestn Otorinolaringol*. 2018;83(3):77-81. [CrossRef]
24. Brown EC, Lucke-Wold B, Cetas JS, et al. Surgical parameters for minimally invasive trans-eustachian tube CSF leak repair: a cadaveric study and literature review. *World Neurosurg*. 2019;122:e121-e129. [CrossRef]
25. Kassam AB, Gardner P, Snyderman C, Mintz A, Carrau R. Expanded endonasal approach: fully endoscopic, completely transnasal approach to the middle third of the clivus, petrous bone, middle cranial fossa, and infratemporal fossa. *Neurosurg Focus*. 2005;19(1):E6. [CrossRef]
26. Prevedello DM, Ditzel Filho LF, Solari D, Carrau RL, Kassam AB. Expanded endonasal approaches to the middle cranial fossa and posterior fossa tumors. *Neurosurg Clin N Am*. 2010;21(4):621-635, vi. [CrossRef]
27. Ikeda R, Miyazaki H, Morita M, et al. Surgical treatments for a case of superior canal dehiscence syndrome associated with patulous Eustachian tube. *Auris Nasus Larynx*. 2019;46(4):630-635. [CrossRef]
28. Takasaki K, Takahashi H, Miyamoto I, et al. Measurement of angle and length of the Eustachian tube on computed tomography using the multiplanar reconstruction technique. *Laryngoscope*. 2007;117(7):1251-1254. [CrossRef]
29. Patel S, Dawood A, Ford TP, Whaites E. The potential applications of cone beam computed tomography in the management of endodontic problems. *Int Endod J*. 2007;40(10):818-830. [CrossRef]

30. Stutzki M, Jahns E, Mandapathil MM, et al. Indications of cone beam CT in head and neck imaging. *Acta Otolaryngol*. 2015;135(12):1337-1343. [CrossRef]
31. Zou J, Lähelmä J, Arnisalo A, Pyykkö I. Clinically relevant human temporal bone measurements using novel high-resolution cone-beam CT. *J Otol*. 2017;12(1):9-17. [CrossRef]
32. Peltonen LI, Aarnisalo AA, Kortesniemi MK, et al. Limited cone-beam computed tomography imaging of the middle ear: a comparison with multislice helical computed tomography. *Acta Radiol*. 2007;48(2):207-212. [CrossRef]
33. Noonan KY, Linthicum FH, Lopez IA, Ishiyama A, Miller ME. A histopathologic comparison of Eustachian tube anatomy in pediatric and adult temporal bones. *Otol Neurotol*. 2019;40(3):e233-e239. [CrossRef]
34. Robert Y, Gaillandre L, Chaillet N, Francke JP. Anatomy of the auditory tube: CT scan and MRI aspect. *Ann Radiol (Paris)*. 1992;35(6):444-452.
35. Leuwer R. Anatomy of the Eustachian tube. *Otolaryngol Clin North Am*. 2016;49(5):1097-1106. [CrossRef]